Huuskonen, Janna; Oksanen, Timo

Soil sampling with drones and augmented reality in precision agriculture

Published in:
Computers and Electronics in Agriculture

DOI:
10.1016/j.compag.2018.08.039

Published: 01/11/2018

Document Version
Publisher's PDF, also known as Version of record

Computers and Electronics in Agriculture 154 (2018) 25–35

Contents lists available at ScienceDirect

Computers and Electronics in Agriculture

journal homepage: www.elsevier.com/locate/compag

Original papers

Soil sampling with drones and augmented reality in precision agriculture

Janna Huuskonen, Timo Oksanen*

Department of Electrical Engineering and Automation, Aalto University, Finland

ARTICLE INFO

Keywords:
Soil analysis
Mixed reality
AR
Precision farming
RPAS

ABSTRACT

Soil sampling is an important tool to gather information for making proper decisions regarding the fertilization of fields. Depending on the national regulations, the minimum frequency may be once per five years and spatially every ten hectares. For precision farming purposes, this is not sufficient. In precision farming, the challenge is to collect the samples from such regions that are internally consistent while limiting the number of samples required. For this purpose, management zones are used to divide the field into smaller regions. This article presents a novel approach to automatically determine the locations for soil samples based on a soil map created from drone imaging after ploughing, and a wearable augmented reality technology to guide the user to the generated sample points. Finally, the article presents the results of a demonstration carried out in southern Finland.

1. Introduction

Today, most of the agricultural field work is carried out with human driven machines in broadacre farming. Because of intensive farming methods in mechanized agriculture, farmers lack hands-on experience with sensing the condition of the field.

Remote sensing methods have been proposed to help in precision farming to gather *data,* and with proper *analytics* the growth during the season can be monitored. More and more satellite imaging data is available during the season. For instance, satellite images from Sentinel-2 satellites are available and provided by European Space Agency (ESA) (Drusch et al., 2012).

Drones, or Unmanned Aerial Vehicles (UAV), or Remotely Piloted Aircraft System (RPAS) are another source for remote sensing. With drones, imaging is possible in cloudy conditions whereas satellite-based imaging is limited in these situations. However, operating with drones requires more effort both in pre-flight phase, flying and the post processing of images than satellite-based imaging. Nonetheless, with satellites, the resolution unit of images is in meters whereas drone imaging has a higher resolution in centimetre-level. (Matese et al., 2015; Bu et al., 2017)

Augmented Reality (AR) is the technology of superimposing virtual objects upon the real world (Azuma, 1997). The virtual content is not limited to visual objects as AR can be used on other senses as well (Azuma, 1997). The benefit of augmented reality is being able to give a user information that is unavailable to their senses and help them perform real-world tasks (Azuma, 1997). While augmented reality may be most familiar from entertainment games, such as Pokémon GO, the application areas of AR include medicine (Fuchs et al., 1998), tourism (Fritz et al., 2005), manufacturing (Caudell and Mizell, 1992) and robot teleoperation (Milgram and Ballantyne, 1997). Today, Augmented Reality equipment is available in the form of wearable glasses.

During recent years, research on using AR in agriculture has emerged. According to Cupiał (2011), AR has several potential application areas in agriculture and in the future, will be an essential tool in precision farming. Santana-Fernández et al. (2010) developed an assisted guidance system for tractors that uses augmented reality with wearable AR technology. As the tractor operates on the field, the parts of the field that have already been treated on are shown in the driver's view on augmented reality glasses (Santana-Fernández et al., 2010). Another navigation system for tractors was developed by Kaizu and Choi (2012) to enable night time farming. Research also suggests the use of AR in identifying pests (Nigam et al., 2011), plants (Katsaros and Keramopoulos, 2017) and weeds (Vidal and Vidal, 2010) and providing the user relevant information based on the identification. Moreover, de Castro Neto and Cardoso (2013) demonstrated the use of AR in a greenhouse. In addition, Liu et al. (2013) state that AR could be used to simulate the growth of crops and livestock, as well as visualize information and help a user to manage different agricultural tasks. Simulation was demonstrated in a study by Okayama and Miyawaki (2013), where an AR smart garden system was developed to teach precision farming concepts to beginners in farming. The system used wearable augmented reality glasses and instructions and plant growth simulations were shown in the user's view (Okayama and Miyawaki,

* Corresponding author at: P.O. Box 15500, Otaniementie 17, 02150 Espoo, Finland.
E-mail address: timo.oksanen@aalto.fi (T. Oksanen).

https://doi.org/10.1016/j.compag.2018.08.039
Received 2 February 2018; Received in revised form 16 June 2018; Accepted 30 August 2018

2013). Okayama and Miyawaki (2013) note that a head-mounted augmented reality device supports farming operations as the user is free to use their hands. Finally, in an application by King et al. (2005), information used for grape production was overlaid against a view of the physical world so that viticulturists could view this information on the grape fields.

In this article, we present a novel concept how to use a drone for soil map colour image acquisition and through automatic segmentation and sampling point selection, the augmented reality glasses guide the farmer to collect the samples representing management zones. For instance, in Finland, the Agri-Environmental Support Programme requires farmers to collect soil samples in a regulated resolution and frequency to receive subsidies (Agency for Rural Affairs Finland, 2018).

The objectives in this article are (a) to study a relevant application of augmented reality in agriculture in practice, (b) to find requirements for drone imaging to acquire valid data for soil mapping, (c) to study the chain of actions to create soil sample points automatically, and (d) to study specific user interface requirements for augmented reality view in the application of assisted soil sampling.

2. Motivation and process chain

2.1. Management zones

A soil map with measured properties is one of the most important data layers when preparing precision farming prescriptions. Even if online soil quality sensors have been developed to measure the soil properties on the fly (Mouazen et al., 2005), the common practice is to collect soil samples and the samples are analysed in a laboratory. For precision farming purposes, the field should be divided into management zones and locations for soil sampling should be selected properly to get information from the zones. Management zones that represent consistent conditions and are similar based on some quantitative measure (Zhang et al., 2002; Fridgen et al., 2004) can be derived from yield maps, satellite images or aerial images or some other measurements. Every soil sample is analysed in a laboratory and the analysis is charged per sample. For this reason, sampling and analysing every square meter of the field would be very expensive and cannot be justified for precision farming purposes. In precision farming, the management zones should be large enough so that the costs of soil sampling and laboratory analysis are lower or equal to the general benefits of precision agriculture, such as additional yield or better quality. In this article, each *management zone* is a uniform region in the field plot that is considered consistent in properties; thus, separated regions with similar properties are considered separate management zones in this article.

Aerial images representing the soil colour can be acquired every year after primary tillage operation. In no tillage farming, the soil is almost always covered by vegetation or crop residues and the colour of the soil cannot be acquired. However, occasionally a field in no tillage farming is ploughed to smooth the surface and after these rare operations, it is possible to acquire images to detect the soil colour.

2.2. Augmented reality

The purpose of augmented reality in this application is to aid the farmer to collect soil samples. The system should not hinder the performance of this task and should be intuitive to use. Moreover, the role of the application should be guiding the user and they should not be required to operate the software. Therefore, input from the real world to the application should be provided as automatically as possible. In addition, the guidance information should come to the user automatically without any need to search for it. Given these requirements, wearable augmented reality glasses are the obvious choice of hardware, as the virtual content will be in the user's view and they are free to operate their hands.

A sample representing a management zone contains several *sample points* that represent the zone. To collect soil from the correct locations, the location of each sample point should be represented to the user. Adding a visual mark to each sample GPS point can be used to illustrate the sites. The state of a sample point must be tracked and represented somehow, as the user must be able to differentiate between already collected and uncollected sample points so that soil is not collected from the same location twice. In addition to the sample point locations, information that supports the operation can be added, such as the amount of already collected samples. However, the user's view should not be cluttered with a multitude of visual cues. The environment should be visible so that the user can navigate the field safely. The information given by the application should be limited to only the relevant instructions and represented in a way that is easy to perceive. Colours can be used to enhance perception.

Augmented reality is not a common tool and is mostly known from entertainment games. While commercial wearable AR equipment today should be comfortable to wear, users may be reluctant to adopt the new technology (Azuma, 1997). To make the application more approachable and intuitive to use, it can be designed to resemble a game.

2.3. Summary of process chain

This article presents a complete working process to make soil maps by utilizing drone and augmented reality technologies. The process chain is presented in Fig. 1.

3. Drone imaging and segmentation

In some regions of the world, soil type varies in a single field plot and these variations are visible in RGB. Therefore, an RGB camera was used for aerial imaging with a drone. For aerial imaging a DJI Phantom 4 Pro (DJI, Shenzhen, Guangdong, China) was used with autopilot

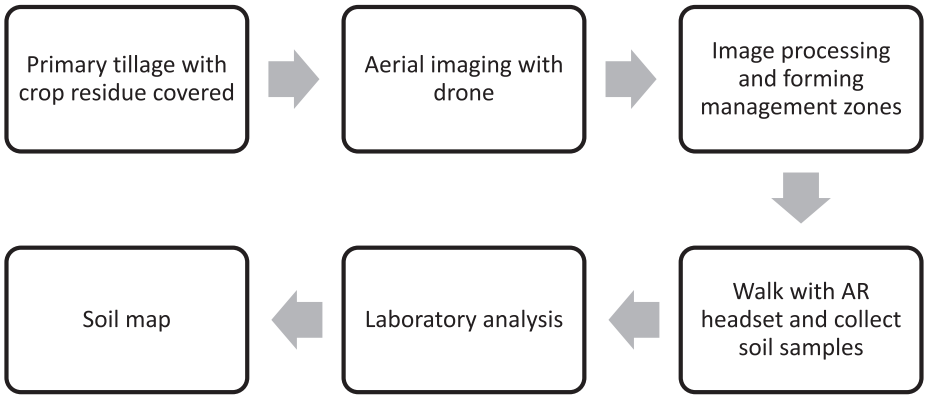

Fig. 1. The process chain presented in the article.

(DroneDeploy, San Francisco, USA) in a tablet.

As the objective in aerial imaging is to see the colour variations of the soil, it is crucial to select the imaging conditions properly, so that (a) the conditions do not change during the flight, (b) shadows and soil surface reflections represent the nominal soil colour and not the moisture variation in the surface and (c) lighting is sufficient for the camera. To avoid biased colours due to varying moisture conditions, the soil should be equally moist and not have standing water on the surface.

The drone used for imaging is equipped with a standard autonomous GNSS receiver without corrections and hence, the position stamps in recorded images are inaccurate. Even if the stitching process done with the DroneDeploy cloud service compensates inaccuracies over dozens of images, the orthophoto is not exactly where it should be as geo referenced image and the deviation may be as large as three meters.

The orthophoto needs to be calibrated into correct position, shape and size. This can be done with landmarks in known positions or a drone equipped with a precise positioning system. In this article, calibration was done manually with some known permanent features in the image, such as electricity poles. After this georeferencing procedure, the image should be clipped so that only the inner area of the field plot remains, to limit colour segmentation only to the soil and not to include any vegetation that has a remarkably different colour. Furthermore, the image may be downsampled to lower resolution, if necessary.

Segmentation of the image into uniform regions is based on a two-stage approach: (a) at the first stage the image is divided into a large number of clusters with SLIC (Simple Linear Iterative Clustering; Achanta et al., 2010) known as superpixels and (b) at the second stage the superpixels are classified into a smaller number of colour classes with K-means clustering (Hartigan & Wong, 1979). In the first stage, the target number of superpixels may be given as a tunable parameter. For the second stage, the K-means algorithm offers more parameters for clustering, such as the number of clusters and the method for calculating distances. Hence, the first stage incorporates spatial clustering and the second stage colour clustering. This segmentation procedure produces the management zones.

The laboratory analysing the soil samples gives instructions on how much soil is collected for each *sample* representing a uniform region. A sample is collected from several scattered locations, known as *sample points*. Each sample point is collected with a tool in the depth of top soil. The area each sample point represents is called a *sample area* in this article.

Finally, the desired number of sample points for each management zone must be automatically generated. For this problem, the SLIC superpixels approach was applied a second time for each management zone, to create equally sized sample areas corresponding to the sample points by iterating the parameter of the superpixels algorithm. Finally, one sample point must be selected per sample area. To find that, it was decided to find the point in the region that is most far point from the boundary of the sample area. To find that point, the watershed algorithm, also known as distance transform, was applied to each region and then peak search. With the watershed-based algorithm, the sample point is guaranteed to be inside the region in any shape.

As the sample points are generated, the visiting order of the regions and the visiting order of the sample points in each region may be sorted to minimize the walking route. This phase is optional. No numeric optimization algorithm was used in this study and the ordering was made manually.

The complete process of image processing phases is presented in Fig. 2.

After image processing, the sample points still lack altitude information. Altitude information for each sample point may be available from GNSS recorded vehicle operations to represent surface profile, or other data source may be used to adjust the altitudes. In this article, a national source for laser scanning data was used to determine the altitude for soil surface. This source is described in chapter 6.3.

4. Augmented reality toolset

4.1. Augmented reality hardware

The smartglasses chosen for this application (ODG R-7 Smartglasses, Osterhout Design Group, San Francisco, USA) are seen in Fig. 3. The glasses are equipped with a small computer running a custom, Android-based operating system by the manufacturer. The glasses use optical see-through technology, as the virtual content is shown on two see-through displays in front of the user's eyes. Thus, the virtual content is partially transparent and seen combined with the view of the user's environment. In addition to visual content, the glasses also have the capacity of haptic feedback in the temples and audio ports that can be used with ear buds.

The ODG R-7 smartglasses include GNSS, Wi-Fi and Bluetooth. The orientation of the user can be detected with an accelerometer, gyroscope and magnetometer, each sensor having 3 axes. In addition, the device has a camera sensor.

User input to the device can be given using a trackpad on the right temple of the glasses. The glasses also include microphones, which could be used to provide input. For power supply, the device has two Lithium-Ion batteries and can be charged with a USB cable. The battery duration depends on the software running on the device. The smartglasses weigh 170 g.

4.2. Augmented reality SDK

Augmented reality software can be developed using a software development kit (SDK) providing functionalities needed for AR. The Wikitude SDK (Wikitude Augmented Reality SDK, Wikitude GmbH, Salzburg, Austria) includes features such as detecting the user's location and orientation, image recognition and geo-locations: rendering virtual content to GPS coordinates. The SDK has a version specifically designed for the ODG R-7 smartglasses and is one of the recommended augmented reality SDKs by the AR device manufacturer. The AR software implemented using Wikitude is written in JavaScript and runs as a browser. The SDK provides methods to implement custom functions for communications between the Android Java code and JavaScript.

4.3. External GNSS receiver

Even if the selected AR hardware has a built-in GNSS receiver, typical for mobile phones, it was decided to use another, more accurate external GNSS receiver for localization. The selected GNSS receiver was a L1 band RTK receiver (Emlid Reach RS, Emlid Ltd, Saint Petersburg, Russia). A correction signal was received from a base station nearby and the position information was transmitted to the AR hardware using the NMEA-0183 protocol over Bluetooth. The GNSS system is able to localize in sub meter accuracy. Finally, only four signals of positioning were used: latitude, longitude and altitude in WGS84 coordinate system and QPS quality (fix), which indicates whether the former are valid. The weight of the selected GNSS receiver is 690 g.

4.4. Software

The developed software is an Android application, written in Java, that uses an augmented reality JavaScript module implemented using Wikitude. The software was developed using the Android Studio IDE.

The main program in Java loads the JavaScript AR module. To utilize the user's location in an Android software, a location provider that receives updates from a device's GPS module is typically implemented. As stated above, in this case, the device's own GNSS was opted out in favour of the more accurate GNSS receiver. As new locations are received, the main program forwards them to the AR module for the use of the Wikitude SDK.

The input data for the smartglasses software from the previous

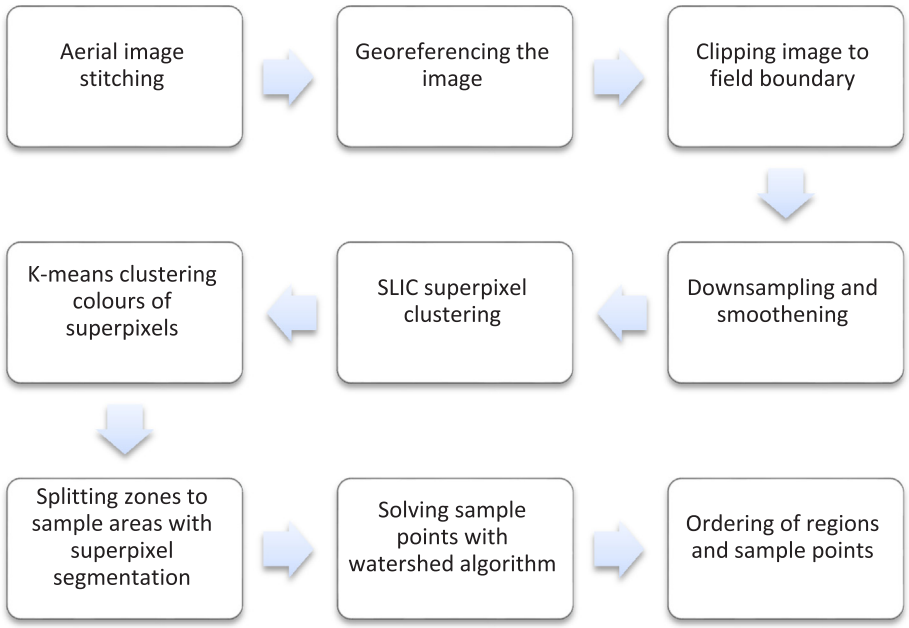

Fig. 2. The phases of the image processing algorithm.

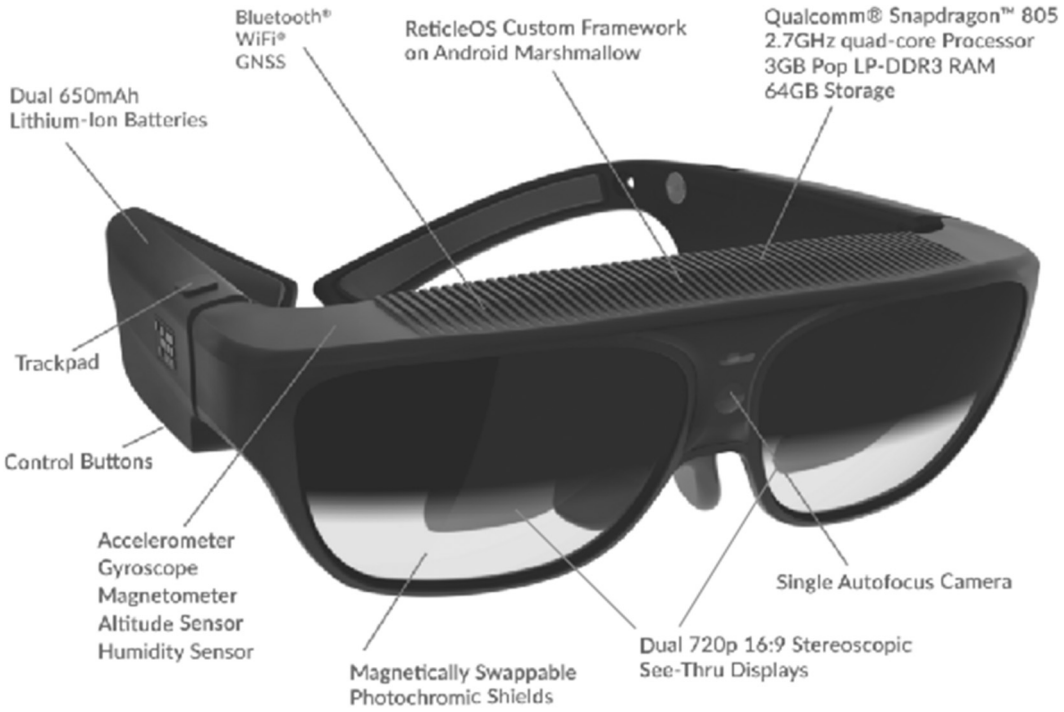

Fig. 3. The augmented reality glasses chosen for the application (ODG R-7, Osterhout Design Group, San Francisco, USA).

phases contains the latitude, longitude, altitude and the region number for each sample point. For each sample point, an ID is created to represent an order number inside the region. This data is stored along with a collect status in the AR module of the software.

As a large field has dozens of sample points, rendering all of them simultaneously may clutter the view. To avoid this, the first sample points in each region are assigned to represent the region and the software keeps track of the active region where the user is currently in. Only the sample points in the current region are shown and for other regions, only a label is shown to indicate the direction of that region. Visible sample points are represented with a 3D object as well as labels with information.

Collecting a sample point is implemented with Wikitude's action range: a GPS location and a radius are given to represent a circular area that does not take altitude into account. If the user's GPS location is within the radius from the GPS location given to the action range, the user is registered as inside the action range. Events can be implemented for the user's entering and exiting the area. Thus, an action range with a predetermined radius is generated for each sample point. As the user enters an action range, a timer starts. If the user stays within the area for a predetermined time, the sample point is marked as collected and if the user exits the area before the timer is done, the sample point is not collected and the area needs to be entered again. In addition to providing a way to signal the program that the sample point is collected

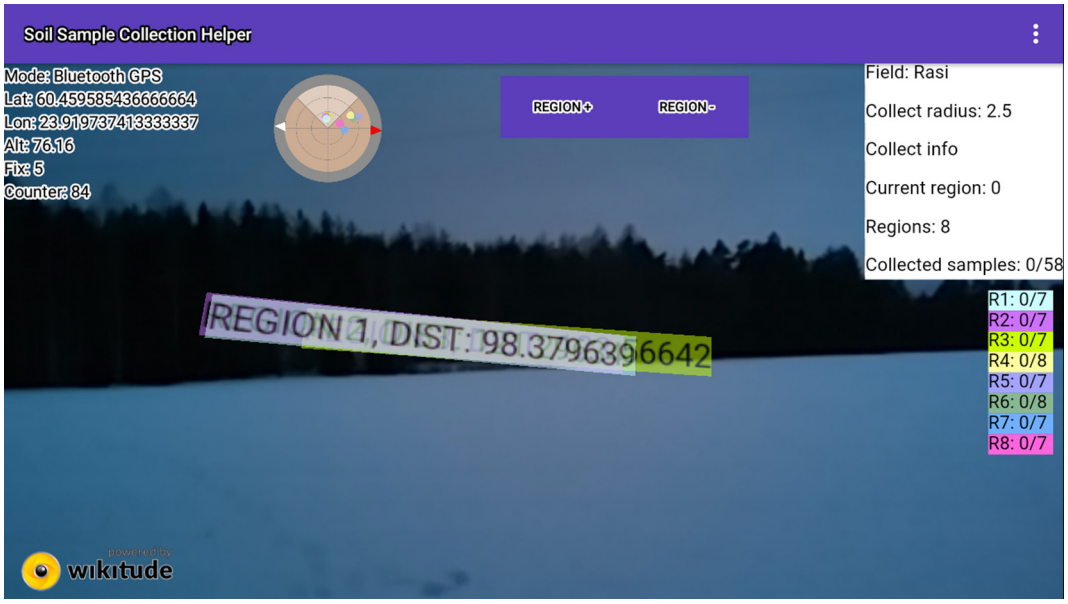

Fig. 4. View seen through the AR smartglasses at the start of the operation.

without manual user input, this implementation is game-like: follow a visual cue and collect it by reaching it.

4.5. The user interface (UI)

A view of the implemented software can be seen in Fig. 4. In the top-left corner, information about the GNSS is shown: the current coordinates of the user from the GNSS receiver, the fix level of the signal and a counter indicating how many location updates the program has received. This is useful in problem situations to verify if the GNSS is inaccurate or has stopped working.

The active region is given by the user by increasing or decreasing the current region using two buttons, marked as "REGION + " and "REGION-". The buttons are operated using the trackpad on the smartglasses. The program starts in region 0, which represents any area outside of the field. As seen in Fig. 4, marks for regions and distances to the regions in meters are shown. Each region has been assigned a colour used to represent it. Additional information is shown in the top-right corner of the view against a white background: the name of the field, the value of the radius parameter used by the action ranges of the sample points, "collect info" which changes depending on the user's actions, current active region, number of regions in total and how many sample points out of total have been collected. In addition, the amounts of collected sample points for each region are listed against background colours corresponding to the region in question. The same colours are used in a radar element shown left of the region buttons. The radar element, a feature in the Wikitude SDK, shows the direction of the North and the approximate field of view of the user. Rendered objects can be represented in the radar. Here, circles are used to represent regions and sample points. The sample points in the active region are shown as smaller circles in the colour of that region and for other regions, a single circle is shown.

Another view from the software can be seen in Fig. 5. In this instance, the active region is region 1, and a sample point is shown in the user's view. To emphasize the game-like experience, a 3D model of a Pokémon (Nintendo, Kyoto, Japan) was chosen to represent the sample point in addition to two labels with the sample point's region, ID, distance to the user and the collect status. In Fig. 5 it can also be seen that one sample point out of the total has been collected and it is from region 1. In addition, the program informs the user that the last activity was collecting sample point 6 from region 1. A collected sample point in an active region is represented with a bright green colour in the radar element so the user can discern between ready sample areas and collectable sample points in their vicinity. To further guide the user to sample points to be collected, a triangle, as seen in bottom-left of Fig. 5, are used to indicate the direction of an uncollected sample point in the active region.

In addition to changing the radar representation when a sample point is collected, it is no more represented with the 3D Pokémon in the user's view but a single label with the sample point's region and number and the status "COLLECTED" on a background of bright green used in the radar element as well. An example of a collected sample point can be seen in Fig. 6. When all sample points in a region are collected, the representation of the region is also changed to indicate this status, as seen in Fig. 7.

5. Experimental setup

The field plot (7.0 ha, 60.4607N 23.9201E) selected for the study was known to contain many soil types such as loam, clay loam, sandy loam and loamy sand. In the optimal situation for imaging, the moisture profile in the soil is consistent and the effect of soil moisture on reflectance is eliminated. In this case, light rain preceded ploughing and therefore, the moisture of the soil had stabilized before the operation. Thus, it was assumed the moisture profile was consistent in the ploughing depth of 20 cm. The light rain continued during the ploughing, so the surface of the field did not dry, which would have biased the colouring of the soil. Furthermore, the plough was tuned properly to make sure that all green matter is hidden, to guarantee nothing else is visible in the image but the bare soil.

The minimum flight altitude in the field was limited by the surrounding forest, and the maximum flight altitude is regulated to 150 m by national law in Finland. To guarantee sufficient quality in the imaging, it was decided to fly near the minimum level. The drone imaging was carried out immediately after ploughing, with standard a DJI Phantom 4 Pro (DJI, Shenzhen, Guangdong, China). The flight altitude was 40 m and resulted in 268 images in 13 min and 40 s.

The sample collection demonstration was conducted December, and there was snow on the ground. Nevertheless, the laboratory used for analysing the samples states that soil samples can be collected as long as the ground is not frozen (Eurofins Viljavuuspalvelu, Mikkeli, Finland).

The hardware used in the demonstration consisted of the

Fig. 5. View seen through the AR smartglasses. A sample point in an active region is shown.

smartglasses, the external GNSS module attached to a backpack, a mobile phone for providing the RTK fix signal and an external power bank for the smartglasses. An external power bank was necessary as the runtime with the internal battery of the smartglasses was 30 min when running the software. The total weight of the equipment and extras was 3.86 kg, including the backpack weighing 2.8 kg. The backpack contained all the materials for soil sampling, such as empty plastic boxes to store soil samples.

The choice of the time parameter, used for marking a sample point as collected, was affected by an estimate of how long it would take to dig a sample and package it into a sample container. Another consideration was how long it would take to be able to pass a sample area without marking it. Thus, the time parameter needed to be large enough to pass the sample areas but short enough to allow continuing the operation as soon as a sample was collected. Based on these factors, the parameter was set to one minute for the demonstration.

6. Results

6.1. Imaging

The aerial images were stitched to a solid orthophoto with the DroneDeploy service (DroneDeploy, San Francisco, USA) to the resolution of 5 cm, and the orthophoto was georeferenced with six precisely known *ground control points* visible in the orthophoto. The surrounding areas in the image were cleared manually, as all around the field green matter (forest, trees or grass) was visible, which was not intended for colour segmentation. Even if the boundary line was precisely known, the boundary clipping was not sufficient as some trees around the field had overhanging branches. The RGB orthophoto is presented in Fig. 8.

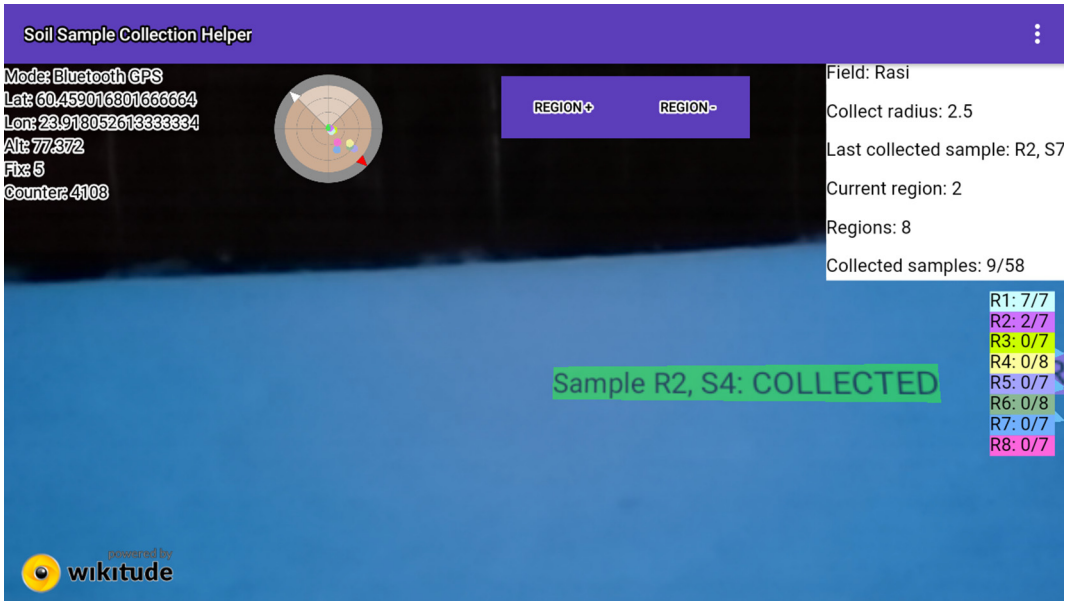

Fig. 6. View seen through the AR smartglasses, showing a label for a collected sample point.

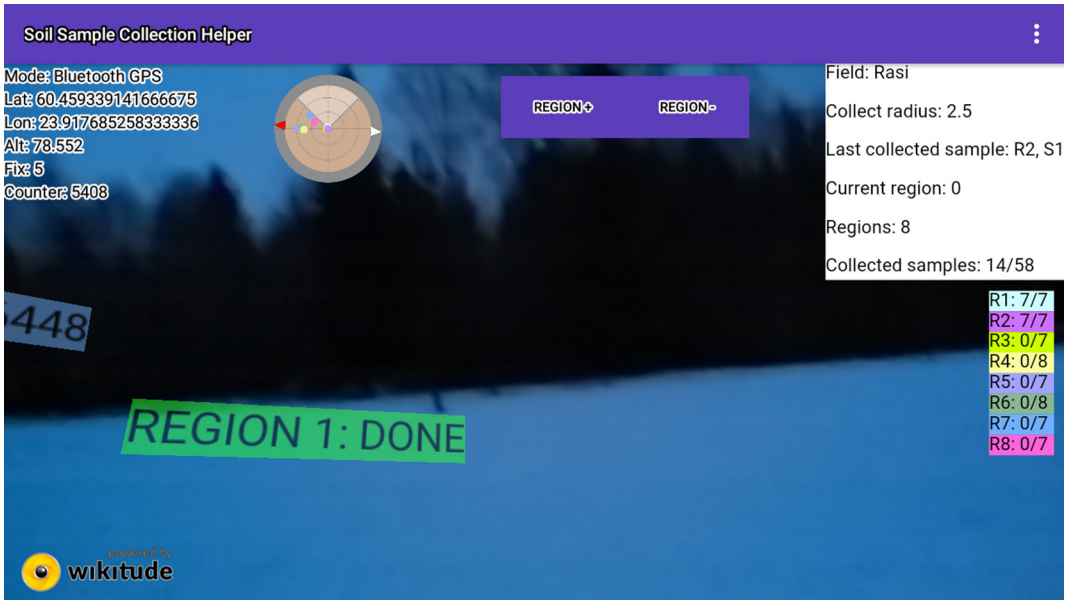

Fig. 7. A completed region in the user's view.

Fig. 8. Stiched, georeferenced and clipped RGB image of the field representing soil colour.

6.2. Segmentation

As described above, the segmentation is based on a two-phase approach. For precision farming purposes, the field (7.0 ha) needs to be divided into several management zones, but practical reasons, including the cost of soil sample analysis and effort to collect those by walking, set a soft upper limit to the management zone size. It was decided that for this field the number of management zones should not be higher than one per hectare, or seven in total, which was considered to be the soft limit.

However, as visible in Fig. 8, the field contains some larger and some smaller consistent regions and thus by trial-and-error, the proper number of management zones was eight, which was acceptable for precision farming requirements. In the SLIC algorithm implemented in Matlab, the target number of superpixels was 40. The average size of superpixels corresponds to half a hectare each, including the areas outside the field in the bounding box. For the K-means clustering, the squared Euclidian distance was used for distance calculation and eight for the number of clusters. Both tuneable parameters (the number of superpixels and the number of clusters) were adjusted by trial-and-error to reach the target average size of a management zone, which was 1 ha in this case. For different sized fields and target zone areas, both parameters need to be adjusted, in a similar manner as contour maps are created for yield maps in commercial precision farming software such as FarmWorks (Trimble Inc., Sunnyvale, USA).

After the first step of segmentation to eight regions, the second step was applied to divide each region into sample areas. The number of sample areas per region was given by the laboratory making the soil sample analysis: the instructions stated that the number of samples per pot was seven or eight (Eurofins Viljavuuspalvelu, Mikkeli, Finland). Thus, this range was given as the rule for sub segmentation. Furthermore, the sample points were solved for each sample area by using the watershed algorithm to find the centre point.

The segmentation result with eight regions, with sample areas and sample points is presented in Fig. 9. The triangle and circle represent the starting and end location for the sampling journey. In total, the map contains 58 sample points in eight regions, 7–8 per region.

6.3. Altitude of sample points

As the previous step resulted in 2D coordinates for the sample points, or latitude and longitude in the WGS84 coordinate system, the altitude must be determined for the field surface. Otherwise, the AR headset would draw the objects deep into the soil or flying above. For the selected field plot, laser scanning data provided by National Land Survey of Finland was available with a spatial resolution of half a point per square meter. The vertical accuracy of the laser scanning data was described as the mean error of 15 cm, which was sufficient for the application. The unfiltered altitude map is presented in Fig. 10, showing the altitude variation of ca. 10 m inside the field. The map also shows

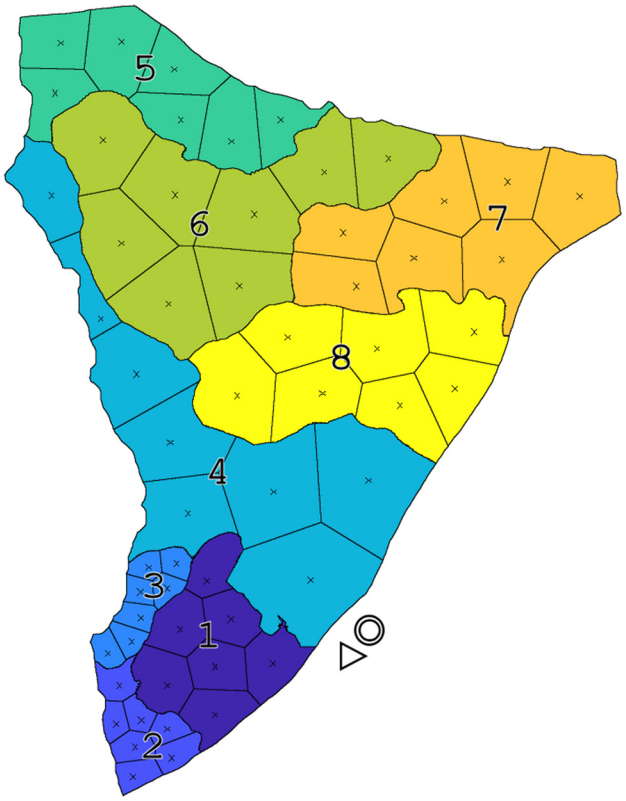

Fig. 9. Segmentation results and sampling areas.

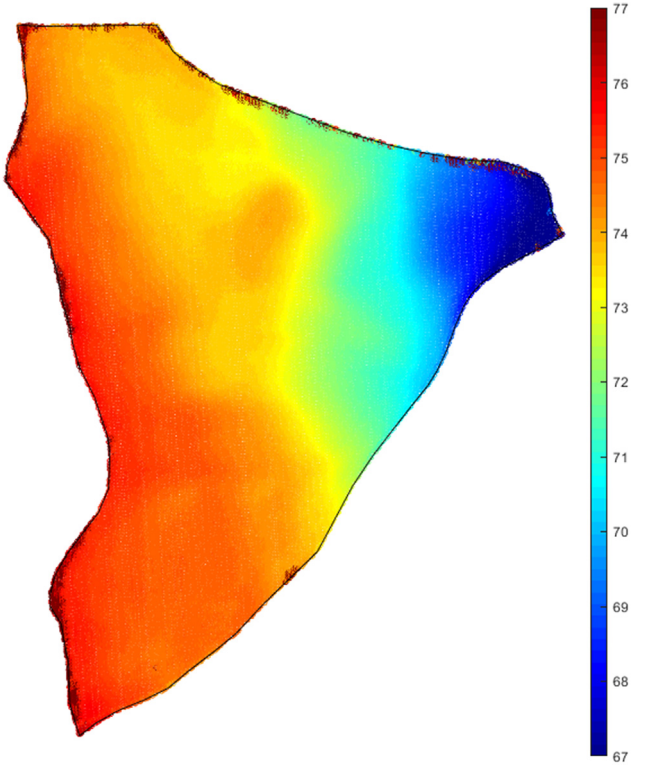

Fig. 10. Geoid altitude of the demonstration field, constructed from the national laser data source. Higher altitudes are marked in red and lower altitudes in blue. The maximum altitude difference in the field was 10 m.

Fig. 11. Regions and walking route to collect 7–8 samples per region.

the surrounding forests and trees, some of which are overhanging the field.

Even though the vertical data was rather accurate, the altitude of the sample points was averaged around each sample point, using a radius of 3 m to average the data of ca. 15 scan points around.

6.4. Sampling order

In the field test, the passing order of regions was determined manually, from 1 to 8. All sample points inside the region were equally shown in the AR display, so the walking order was not forced. The walking order of sample points is presented in Fig. 11.

6.5. User experience

Collecting the samples started in region 1 and the regions were traversed in increasing order. As the order of collection was not forced, the sample points were collected in an order chosen by the authors. This resulted in a suboptimal route, as the shortest order to traverse the sample areas was difficult to estimate from the UI and was based on the distance readings of the sample points. The distance readings were important to navigate and determine how close a sample point was even though when the sample area was reached, it was possible to stand on top of the virtual mark and collect the sample point from that location. An example of the suboptimal order of traverse can be seen in Fig. 12, where the user collected sample point 6 of region 4 after sample 3, then doubling back to collect sample point 2.

The sample points were easy to find even though the direction where the sample point was seemed to change when nearing the sample area. This was because of the magnetometer: based on the radar element, the direction of the North given by the smartglasses seemed to be off. This resulted in the user first aiming to a slightly incorrect direction and then making a turn to reach the sample area when it was close. This can be seen in Fig. 13, in which the user's path is plotted in blue and the sample points are marked with 'x'.

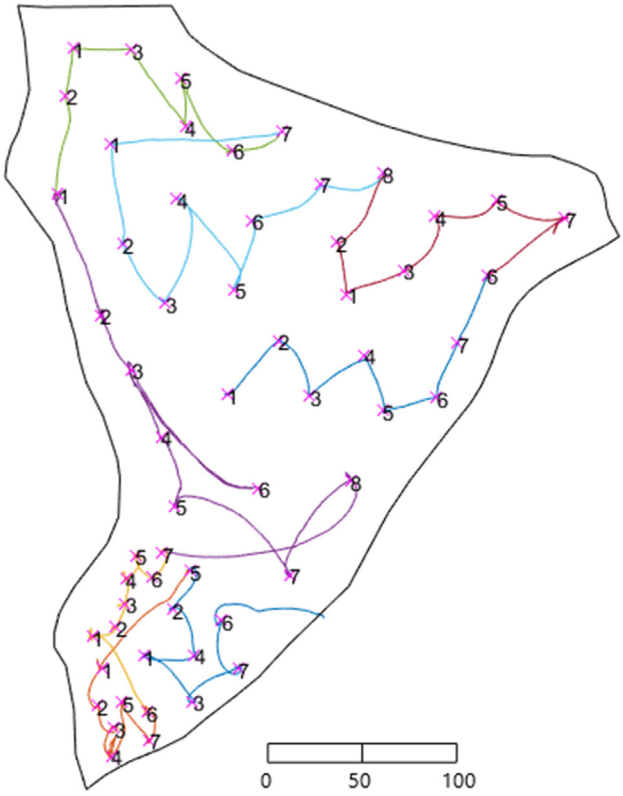

Fig. 12. The GPS route the user took to collect the samples and the sample locations. Regions are represented with different colours and the samples are numbered. The scale is in meters.

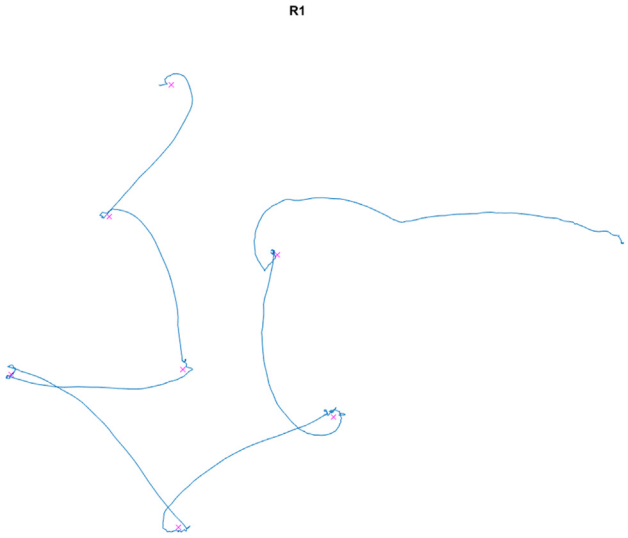

Fig. 13. Walking record in Region 1. The solid line represents the route of the user and the crosses illustrate the sample points.

Table 1
Magnetometer hard iron bias values before and after calibrations done in region 2.

	Before	After
Bias X	−19.5	−20.63
Bias Y	30.56	22.25
Bias Z	22.25	16.31

Table 2
Magnetometer hard iron bias values before and after calibration done in region 4.

	Before	After
Bias X	−20.63	−20.94
Bias Y	22.25	24.19
Bias Z	16.31	17.31

To improve the orientation detection by the smartglasses, calibration of the magnetometer was done by rotating the glasses in a Fig. 8 pattern. Calibration was done first four times in region 2, and the procedures changed the hard iron bias values, as seen from Table 1. Calibration was done several times in a row because the first calibrations did not seem to improve the situation.

The user's experience was that the direction of north improved after the last calibration. The change in the bias Y value seems to support this: in these smartglasses, the Y-axis points up and thus, is the yaw axis. While this calibration fixed the worst offsets, a small offset in the direction of the North was still observed by the user. Thus, calibration was attempted again in region 4, and as can be seen in Table 2, the procedure resulted in only small changes. The observation of the user was that the small offset was not corrected by calibration, and these values support the observation.

The GNSS worked most of the time but in some instances, the GNSS shifted while a sample point was collected, resulting in the user exiting the action range of the sample point and needing to find the sample area again to activate the timer. This resulted in a waste of time and as the GNSS kept jumping, the sample area needed to be chased to stay within the radius. In addition, some sharp changes in altitude were experienced, to such a degree that the sample points seemed to be several meters above or under the user. These occurrences, however, lasted for two minutes at the longest and did not prevent the work.

Overall, the developed AR application provided the planned functionality and guided the user to all the sample areas. The only manual user input needed was changing the regions, as the sample points were marked as collected automatically. Each sample point was collected within the predetermined radius, which was 2.5 m. Information in the user interface was useful: the collect information indicated when a sample point was in the process of being collected, which was essential during the GNSS jumping. While the amounts of collected sample points were helpful to track the progress of the work, the radar element did not provide the usefulness in navigation that was planned, as the points in the radar were too close to each other to differentiate clearly. The radar, however, was essential for determining when calibration of the magnetometer was needed.

6.6. Soil map results

The collected samples were analysed in the laboratory for agricultural soil samples (Eurofins Viljavuuspalvelu, Mikkeli, Finland). The results contain information on soil type, pH and contents of Ca, P, K, Mg and S. pH was almost equal in all management zones (between 6.1 and 6.9). The phosphorus concentration (P) was more varying and this is illustrated in Fig. 14.

7. Discussion

The drone used for imaging was a DJI Phantom 4 Pro, which was the top model in the series of small consumer drones at the time. The quality of the camera in the drone was sufficient for soil mapping. For the experimental setup, a 40-m flight altitude was chosen. However, a higher altitude could also have resulted in a sufficient quality for the application with a shorter flight time.

For the AR application, a better scaling of the size of the virtual

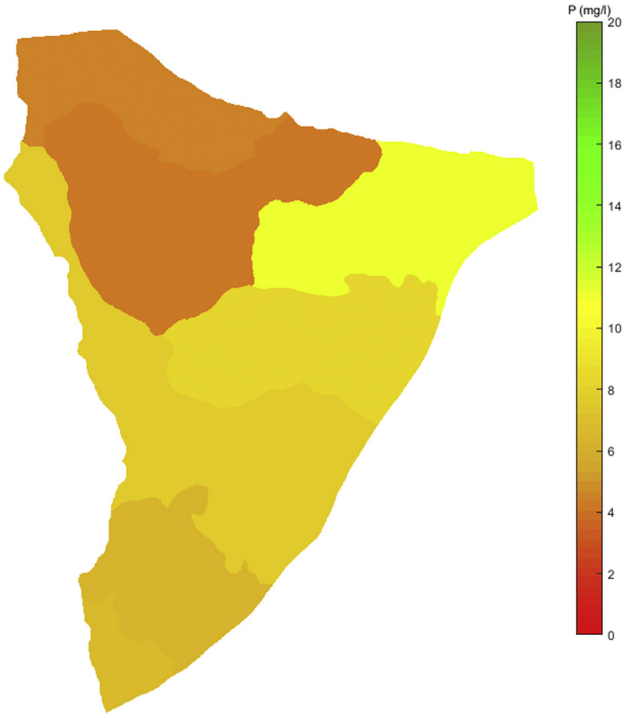

Fig. 14. Phosphorus content in the field per management zone, based on lab analysis of the samples collected from the demonstration field.

objects is needed as it was difficult to estimate distances to the sample areas based on the sizes of the marks and thus, navigation relied on the distance readings. Wikitude scales the virtual objects based on the user's distance to them but in addition, a scale value can be given to the objects to adjust how large they are in the user's view. Based on this test, more experimentation with this value is needed. As seen in Fig. 15, the objects appeared to be closer to the user than what the distance values indicate, and thus, should be scaled to look smaller. Another scaling factor to improve is the radar size, as the objects in the radar were not easily distinguishable. As earlier tests utilized a much smaller test field, the size of the radar should have been scaled to match the larger size of the field.

As stated above, the order in which the sample points were collected was not optimal for the user and therefore, a recommended order of traverse should be represented by the software. This could be done using colours, showing only one sample point at a time or showing a map of the field, similar to Fig. 11 with the sample point IDs and the order of traversal marked by a line. This map view could fit for example under the GNSS information in the UI.

The 2.5-m radius of the action range was appropriate as long as the GNSS was accurate. Besides the radius, another parameter affecting how a sample point is collected is the time needed to stay within the action range. As mentioned above, this parameter was set to one minute. This time was experienced to be too long, as for approximately 70% of the cases, the sample point was collected before the timer had run out and the user had to wait before advancing towards the next sample point.

The AR content in this application was purely visual. However, the used hardware enables sound input and output as well as haptic feedback. A future improvement on the software could be using speech recognition as a user input means to eliminate any need to operate the application with hands, as well as provide sound and haptic feedback on events such as collecting a sample point.

As the demonstration was held in winter, the amount of sunlight was limited. The amount of light could affect the visibility of the AR content and thus, replicating the demonstration during summer time might require using tinted shields for the smartglasses.

The altitude of the sampling points was determined from the laser scanning data available. The vertical accuracy for the user experience depends on the accuracy of the terrain model and the altitude of the sample points as well as on the vertical accuracy of GNSS. The user experience was good when it comes to altitude when the GNSS was properly positioning, and the objects were smoothly on the surface of the field. In earlier tests, a GNSS receiver without a fix was used, resulting in altitude variations of tens of meters within seconds, making the virtual objects almost impossible to track.

As the imaging of soil is crucial to get a proper map, it could be even recommended that the ploughing/primary/secondary tillage tractor is equipped with a small drone. This would allow that when the field is completed, the first imaging could be done immediately and if the quality is not sufficient, imaging must be done another time.

One could automate the soil sampling itself by robotics, as proposed by Cao et al. (2003). The approach proposed in this article is valid for

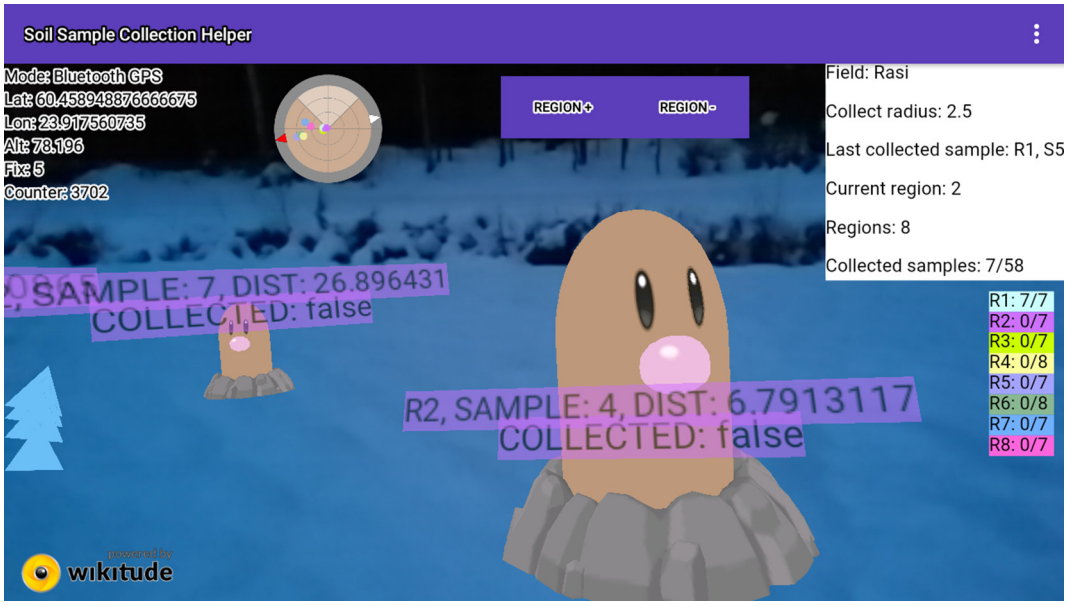

Fig. 15. View seen through the AR smartglasses. The distance to the locations indicated by the virtual marks does not match how they are perceived in the view.

creating the sampling points, but for navigation, the autonomous vehicle would need additional information, such as the location of obstacles and other terrain impassable. For a human being who has been on the field, navigation is natural and it is not necessary to create a full traverse map. As mentioned earlier, the farmer rarely walks in the field to see the soil and we think it is valuable to collect the samples manually as for example in Finland, the farmers have more and more reporting responsibility to describe the soil condition for the administration.

8. Conclusions

In this article, a complete chain of actions from ploughing to soil sample analysis was presented to create a top soil map with management zones for precision farming purposes.

In imaging with drones, it was discovered that the soil moisture must be consistent, and the lighting condition must be such that the soil reflection corresponds to the colour, not e.g. to the shininess of clay after ploughing or a 3D pattern of the soil surface after ploughing or shadows.

The user interface of the AR application was feasible and guided the user to all the sample areas. It was possible to collect sample points while using the application, and the application needed little input from the user. Some improvements can be made to enhance the user experience.

The GNSS of the smartglasses is not accurate enough for this application, and a GNSS receiver with a fix signal is needed. Moreover, navigating the field is impossible if the hardware detects the user's orientation incorrectly, making the accuracy of the magnetometer crucial. Overall, the chosen AR hardware was suitable for this application.

The Wikitude augmented reality SDK provided the necessary functionality to render content to GNSS points as well as essential features that enhanced the user experience.

The soil analysis revealed some variation between the management zones, especially in nutrient contents, and further steps towards precision farming application rate control will be studied in the future.

Acknowledgements

The research was funded by the Academy of Finland, decision number 306025.

References

Achanta, R., Shaji, A., Smith, K., Lucchi, A., Fua, P, Süsstrunk, S., 2010. Slic Superpixels. Technical Report 149300, EPFL Technical Report No. 149300.

Agency for Rural Affairs, Finland. Environment payment commitment terms. < http://maaseutuvirasto.mobiezine.fi/zine/370/article-28415 > .(Online accessed May 23rd 2018, in Finnish).

Azuma, R., 1997. A survey of augmented reality. Presence: Teleoperators and Virtual Environments, 6(4), 355–385.

Bu, H., Sharma, L.K., Denton, A., Franzen, D.W., 2017. Comparison of satellite imagery and ground-based active optical sensors as yield predictors in sugar beet, spring wheat, corn, and sunflower. Agron. J. 109, 299–308.

Cao, P., Hall, E., Zhang, E., 2003. Soil sampling sensor system on a mobile robot. In: Proceedings of SPIE Intelligent Robots and Computer Vision XXI: Algorithms, Techniques and Active Vision, Vol. 5267, pp. 304–310.

Caudell, T.P., Mizell, D.W., 1992. Augmented reality: an application of heads-up display technology to manual manufacturing processes. In: Proceedings of the Twenty-Fifth Hawaii International Conference on System Sciences, Kauai, HI, USA, pp. 659–669.

Cupiał, M. 2011. Augmented reality in agriculture. In: Proceedings of the V International Scientific Symposium: Farm Machinery and Process Management in Sustainable Agriculture, Lublin, Poland, pp. 23–24.

de Castro Neto, M., Cardoso, P., 2013. Augmented Reality Greenhouse. In: Proceedings of EFITA2013: Sustainable Agriculture through ICT innovation.

Drusch, M., Del Bello, U., Carlier, S., Colin, O., Fernandez, V., Gascon, F., et al., 2012. Sentinel-2: ESA's optical high-resolution mission for GMES operational services. Remote Sens. Environ. 120, 25–36.

Eurofins Viljavuuspalvelu, Mikkeli, Finland. Guidelines for collecting soil samples. < https://cdnmedia.eurofins.com/european-east/media/1667937/maanaytteiden_otto-ohjeet.pdf > (Online Accessed June 15th, 2018, in Finnish).

Fridgen, J.J., Kitchen, N.R., Sudduth, K.A., Drummond, S.T., Wiebold, W.J., Fraisse, C.W., 2004. Management zone analyst (MZA). Agron. J. 96 (1), 100–108.

Fritz, F., Susperregui, A., Linaza, M.T., 2005. Enhancing cultural tourism experiences with augmented reality technologies. In: Proceedings of the 6th International Symposium on Virtual Reality, Archaeology and Cultural Heritage (VAST), Pisa, Italy.

Fuchs, H., Livingston, M.A., Raskar, R., Colucci, D., Keller, K., State, A., Crawford, J.R., Rademacher, P., Drake, S.H., Meyer, A.A., 1998. Augmented reality visualization for laparoscopic surgery. MICCAI '98 919–930.

Hartigan, J.A., Wong, M.A., 1979. Algorithm AS 136: A K-means clustering algorithm. J. Roy. Statist. Soc. C Series 28 (1), 100–108.

Kaizu, Y., Choi, J., 2012. Development of a tractor navigation system using augmented reality. Eng. Agric. Environ. Food 5 (3), 96–101.

Katsaros, A., Keramopoulos, E., 2017. FarmAR, a farmer's augmented reality application based on semantic web. In: Proceedings of the 2017 South Eastern European Design Automation, Computer Engineering, Computer Networks and Social Media Conference (SEEDA-CECNSM), pp. 1–6.

King, G.R., Piekarski, W., Thomas, B.H., 2005. ARVino – Outdoor Augmented Reality Visualisation of Viticulture GIS Data. In: Proceedings of the Fourth IEEE and ACM International Symposium on Mixed and Augmented Reality, pp. 52–55.

Liu, M., Li, X., Lei, X., Wu, S., 2013. Research of mobile augmented reality technology applied in agriculture. In: Proceedings of the International Conference on Advanced Computer Science and Electronic Information (ICACSEI 2013), Beijing, China, pp. 311–315.

Matese, A., Toscano, P., Di Gennaro, S.F., Genesio, L., Vaccari, F.P., Primicerio, J., Belli, C., Zaldei, A., Bianconi, R., Gioli, B., 2015. Intercomparison of UAV, aircraft and satellite remote sensing platforms for precision viticulture. Remote Sensing 7 (3), 2971–2990.

Milgram, P., Ballantyne, J. 1997. Real world teleoperation via virtual environment modelling. In: Proceedings of the International Conference on Artificial Reality and Tele-existence, pp. 1–9.

Mouazen, A., de Baerdemaeker, J., Ramon, H., 2005. Towards development of on-line soil moisture content sensor using a fibre-type NIR spectrophotometer. Soil Tillage Res. 80 (1–2), 171–183.

Nigam, A., Kabra, P., Doke, P. 2011. Augmented reality in agriculture. In: Proceedings of the IEEE 7th International Conference on Wireless and Mobile Computing, Networking and Communications (WiMob), pp. 445–448.

Okayama, T., Miyawaki, K., 2013. The "Smart Garden" system using augmented reality. IFAC Proc. Volum. 46 (4), 307–310.

Santana-Fernández, J., Gómez-Gil, J., Del-Pozo-San-Cirilo, L., 2010. Design and implementation of a GPS guidance system for agricultural tractors using augmented reality technology. Sensors 10 (11), 10435–10447.

Vidal, N.R., Vidal, R.A., 2010. Augmented reality systems for weed economic thresholds applications. Plantadaninha 28 (2), 449–454.

Zhang, N., Wang, M., Wang, N., 2002. Precision agriculture—a worldwide overview. Comput. Electron. Agric. 36 (2–3), 113–132.